Trop J Nat Prod Res, January 2026 10(1): 6799 - 6810 **ISSN 2616-0684 (Print)**
ISSN 2616-0692 (Electronic)

Tropical Journal of Natural Product Research

Available online at https://www.tjnpr.org

Original Research Article

Bidens pilosa Leaves Attenuate Alcohol Induced Chronic Kidney Injury: *In Silico* and *In Vivo* Studies

Melva Silitonga[1]*, Putri Windah Sinaga[1], Herbert Sipahutar[1], Hendro Pranoto[1], Adriana Yulinda Dumaria LumbanGaol[1], Feimmy Ruth Pratiwi Sipahutar[1,2], Erlintan Sinaga[1], Fajar Apollo Sinaga[3]

[1]*Department of Biology, Faculty of Mathematics and Natural Sciences, Universitas Negeri Medan, North Sumatra, Indonesia;*
[2]*Bioinformatics Research Group, Department of Chemistry, Faculty of Mathematics and Natural Science, Universitas Indonesia, Depok, Indonesia;*
[3]*Department of Sports Studies, Universitas Negeri Medan, North Sumatra, Indonesia*

ARTICLE INFO

Article history:
Received 19 September 2025
Revised 23 December 2025
Accepted 25 December 2025
Published online 01 January 2026

ABSTRACT

Excessive alcohol drinking leads to chronic kidney injury (CKI). *Bidens pilosa*, as a medicinal plant, has promising antibacterial, antimalarial, hepatoprotective, and antidiabetic activities. There is a dearth of information on the therapeutic effect of ethanol extract of *Bidens pilosa* leaves (EEBP) against alcohol-induced CKI. The exploration of EEBP as renoprotection was evaluated through a comprehensive experimental and pharmacoinformatics analysis. Alcohol (10 ml/kg) was administered for 6 weeks or in combination with EEBP (250, 500, and 750 mg/kg). Induction of alcohol significantly ($p \leq 0.05$) increased the total cholesterol, triglyceride, LDL, creatinine, and uremic levels. Furthermore, kidney tissue abnormalities were observed in the alcohol group. The data indicated that EEBP improved the kidney histology and decreased the levels of lipid profile and kidney function parameters. The compounds have the flexibility and stability to bind to active sites of protein, consisting of PPARG, SIRT, HIF1A, and NQO1. This study shows that EEBP exerted an ameliorative effect in alcohol-induced kidney injury.

Keywords: *Bidens pilosa*, Kidney, Alcohol, Docking, pharmacoinformatic

Introduction

Chronic alcohol intake has a higher morbidity and mortality due to the dysfunction of the kidneys.[1] The alcohol dehydrogenase (ADH) plays an important role in converting alcohol to acetaldehyde, which could be toxic in cells.[2] The development of cancer with alcohol intake is associated with the ADH1B gene. The kidney function damage was related to nephrotoxicity.[3] Based on the previous study, it has been stated that primary kidney disorders accelerated by continuous alcohol consumption tend to cause a decreased the rate of glomerular filtration at 7 mL/min/1.69 m^2. [4] High-dose alcohol metabolism increases the nicotinamide adenine dinucleotide (NADH), lipid oxidation, and free radicals. [5] The imbalance of antioxidant agents[6], for example NAD(P)H quinone dehydrogenase-1 (NQO1), could be an indicator for the rise of alcohol dehydrogenase activity that is linked to the excessive TGF-β transcription.[7] In addition, the accumulation of alcohol disrupts 11β-hydroxysteroid dehydrogenase activities in the kidney.[8] This enzyme is involved in blood pressure regulation and the mineralocorticoid receptor in the kidney.[9] The previous evidence reported that higher alcohol intake decompensated 75% of cirrhosis associated with glomerulopathy.[10] Although numerous studies have reported that CKI prevalence correlated with heavy alcohol intake[11-13], the mechanisms of the ameliorative effects of medicinal plants on CKI therapy are unknown.

*Corresponding author. E mail: melvasilitonga@unimed.ac.id
Telp: +62 813 7516 4202

Citation: Silitonga M*, Sinaga PW, Sipahutar H, Pranoto H, LumbanGaol AYD, Sipahutar FRP, Sinaga E, Sinaga FA. Bidens pilosa leaves attenuate alcohol induced chronic kidney injury: *in silico* and *in vivo* studies. Trop J Nat Prod Res. 2026; 10(1): 6799 – 6810 https://doi.org/10.26538/tjnpr/v10i1.51

Official Journal of Natural Product Research Group, Faculty of Pharmacy, University of Benin, Benin City, Nigeria

Bidens pilosa is a medicinal plant used for managing several diseases, for instance, gastritis, pharyngitis, diarrhea, smallpox, colic, infectious disease and asthma.[14] *B. pilosa* leaves have higher antioxidants that tackle scavenge free radicals.[15] Prior studies documented that the constituents of *B. pilosa*, consisting of phenylpropanoids, flavonoids, aliphatic compounds, porphyrins, terpenes, and flavonoids, have significantly decreased the risk of diabetes, hypertension, and hyperglycemia.[16] Based on pharmacological activities, the EEBP has some properties, such as anti-carcinogenic, anti-mutagenic, hepatic disorder treatment, immunomodulatory, and anti-inflammatory.[17]

Treatments for CKI are usually associated with undesirable effects.[18,19] There are limited studies on the biological mechanisms of EEBP would attenuate the kidney disorder after administration of alcohol and construct the molecular pathway of CKI treatment.

Methods

Plant Authentication

Bidens pilosa leaf was procured from Jae Village (GPS Code: 6MJW568P+HH, North Sumatera, Indonesia) on March 12, 2025. The classification process was done by a taxonomist the Biology Laboratory, State University of Medan, Indonesia.

Extraction of B. pilosa leaves

100 g of sample was rinsed, dried and powdered to the mesh size. The maceration was adjusted utilizing ethanol solvent (89%) with twice-a-week intermittent shaking. The extract was refined, concentrated by a rotary evaporator, and stored at 4^0C.

In vivo studies in rats

The Institutional Ethics Committees of UNIMED approved all animal treatment regulations (ethical ID 0453/KEPH-FMIPA/2019). The animal protocols followed the guidelines of 2010/63/EU. This study was executed for six weeks using twenty-five male rats (180 ± 30 g) (n=5). The rats were treated as follows: the group T0 was administered CMC 0.5%; group T1 was given orally 32% alcohol 10 ml/kg; group T2 received 32% alcohol (10 ml/kg) + EEBP 250 mg/kg; group T3 was given 32% alcohol 10 ml/kg + EEBP 500 mg/kg; group T4 was administered 32% alcohol 10 ml/kg + EEBP 750 mg/kg. On the last

ISSN 2616-0684 (Print)
ISSN 2616-0692 (Electronic)

experiment day, all the animals were anesthetized using chloroform had had their neck dislocated, and were dissected in the abdominal cavity. The blood was put in the tube with an ethylene diamine tetra acetic acid (EDTA). The isolated kidneys were collected, weighed, and put into the tube with 10% formalin neutral buffer.

Biochemical analysis
The blood was centrifuged at 3000 rpm for 5 minutes. Serum total cholesterol, triglyceride, HDL, and LDL were evaluated using commercial biochemical kits (PT. Rajawali Nusindo, Indonesia). The creatinine and uremic level were determined using a photometric method.

Histology staining
The pathological alterations in kidney tissues were observed using the H&E method. The samples were dehydrated, cleared, infiltrated, and embedded based on our previous research. [20] Tissue sections were photographed under magnification of 100x using a light microscope (Nikon E400, Sanford).

Data Analysis
All distributed values were shown as mean ± standard deviation (SD). Statistical evaluation was compared with ANOVA followed by post hoc Tukey's test. $p \leq 0.05$ was considered the significant difference.

Modern Pharmacological Identification
The phytocompounds from *B. pilosa* and gene markers of CKI were exported to the STRING database. The confidence score of 0.7 was set to predict the signal pathway between protein and active compounds of the species "*Homo sapiens*". Protein network construction was demonstrated utilizing Cytoscape ver. 3.9.1. [21]

Docking Study
The compounds of EEBP were extracted from the PubChem database. All protein structures (3D), for instance PPARG, SIRT, HIF1A, and NQO1 [22], were downloaded from the RCSB database. AutoDockTools 1.5.7 was employed to clean the water and ligands from the protein structure. Autodock Vina software ver. 4.2 was applied to facilitate the docking study. The interaction between the receptors and compounds of *B. pilosa* complexes was rendered using Biovia Discovery Studios software.

Dynamic Simulation
The conformational ensembles were predicted using molecular dynamic simulation.[23] The Cabs-flex database was utilized to perform the protein stability motion.[24] RMSF scores determined the dynamic of flexible regions between the active compounds of *B. pilosa* and receptors.

Results and Discussion

The metabolism of alcohol generates the accumulation of superoxide radicals, ROS, and hydrogen peroxide.[25] Continuous alcohol intake could raise pro-inflammatory activities and oxidative injury.[26] High ROS production affects antioxidant activities and mitochondrial impairment in the kidney cells.[27] This evidence alters the vasopressin secretion and electrolyte balance [28,29], which results in diuresis and hyponatremia. [30,31] The urinary antioxidant capacity[32] affected the kidney function[33] through the elimination process of hydroxyl, singlet oxygen, and peroxyl radicals.[34] In this current study, the alcohol model of kidney injury was created to identify the beneficial effect of EEBP through pharmacoinformatic and *in vivo* analysis. The alcohol rats (T1) indicated the highest of oxidative injury markers in the kidney. In contrast, the EEBP supplementation (500 and 750 mg/kg) significantly reduced ($p \leq 0.05$) total cholesterol, triglyceride, creatinine, uremic, and LDL levels (**Figure 1**). Compared to group T0, a significant reduction ($p \leq 0.05$) of HDL was performed in the alcohol groups. Group T3 significantly increased the HDL level. This finding is consistent with the previous investigation that the medicinal plant could suppress the renal fibrosis and dysfunction in the mice model of CKI.[35]
Additionally, histoarchitecture examination of kidney tissues showed the normal distal tubular and renal proximal structures in the control groups (T0). In contrast, the significant histological abnormalities were found in the alcoholic groups (T1); for instance, the inflammatory cell infiltration, tubule interstitial fibrosis, Bowman's capsule dilatation, and glomerular shrinkage (**Figure. 2**). Morphological alteration of the glomeruli could be the primary indicator in chronic kidney progression.[36–38] The treatment of EEBP at doses of 500 and 750 mg/kg, respectively, indicated reduced distortions in kidney histology due to fewer areas of tubular epithelial loss, Bowman's space dilatation, and cellular inflammation.

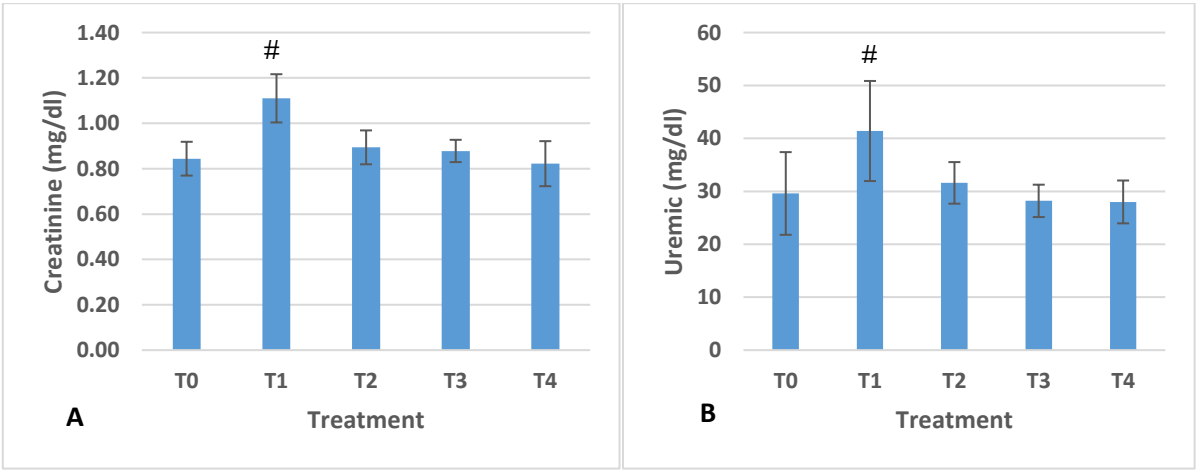

ISSN 2616-0684 (Print)
ISSN 2616-0692 (Electronic)

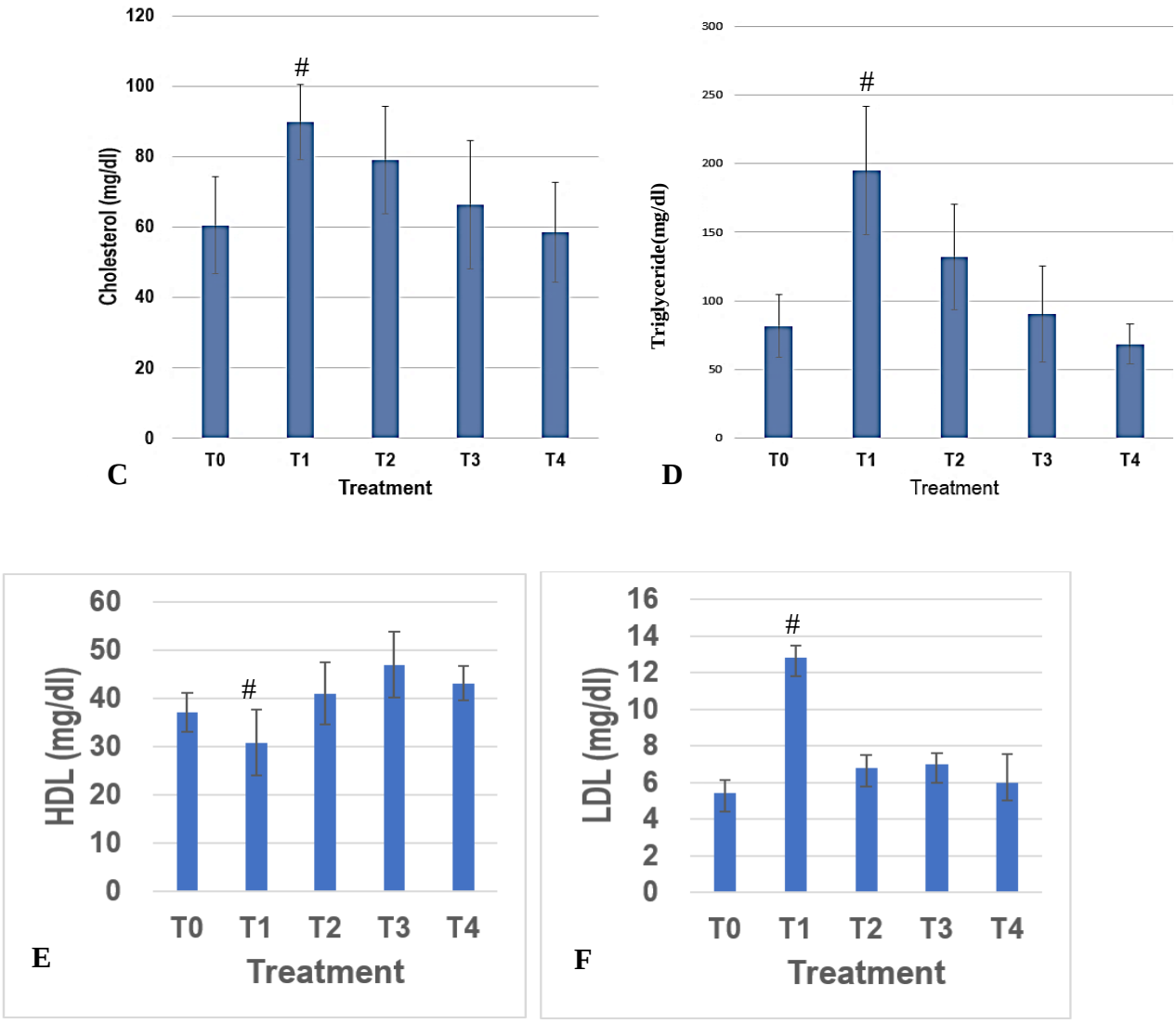

Figure 1: Effect of EEBP supplementation on the level of (A) Creatinine, (B) Uremic; (C) Cholesterol; (D) Triglyceride; (E) HDL; and (F) LDL in alcohol-induced kidney injury. T0 (CMC 0.5%); T1 (30 % alcohol 10 ml /kg); T2 (30 % alcohol 10 ml /kg + EEBP 250 mg /kg); T3 (30 % alcohol 10 ml /kg + EEBP 500 mg /kg); T4 (30 % alcohol 10 ml /kg + EEBP 750 mg /kg). ($^{\#}p \leq 0.05$, n=5.

The current research claimed 79 nodes and 901 edges in the protein network construction between *B. pilosa* and alcohol kidney injury. The Cytoscape software identified 13 core targets (Figure 3A), which had a higher level, including TP53, AKT1, SIRT1, JUN, MAPK8, NQO1, KRAS, PPARG, MTOR, HIF1A, MAPK3, IL6, and FOS. As depicted in Figure 3B, the top 10 are the relevant biological enrichments of the core target linked to CKI, notably the response to reactive oxygen species and cellular response to chemical stress. The significant mechanism pathway of *B. pilosa* relieved the CKI in alcohol rats is illustrated in Figure 3C.

For a strong investigation of the therapeutic effect of EEBP, pharmacoinformatic approaches[39] have been employed to verify the possible molecular mechanism of EEBP in alcohol-induced CKI. Furthermore, the docking analysis verified the potential of EEBP with a higher binding affinity to the active site of PPARG, SIRT, HIF1A, and NQO1, as presented in Figure 4. A total of 7 active compounds from *B. pilosa*, such as, apigenin, apigenin-7-apioglucoside, lupeol acetate, daucosterol, luteolin, quercetin, and lupeol acetate (Table 1), have a good binding pose and a low docking score. Additionally, the dynamic simulation data revealed the structural flexibility between the active phytocompounds of *B. pilosa* and the core target complexes, as shown in Figure 5. The optimization of novel therapy for CKI via molecular mechanism evaluation tends to enhance the efficacy and effectiveness of treatments[40], for example, the development of pharmacoinformatic strategies through the enhancement of integrin β1/JNK signaling transduction in CKI.[41]

ISSN 2616-0684 (Print)
ISSN 2616-0692 (Electronic)

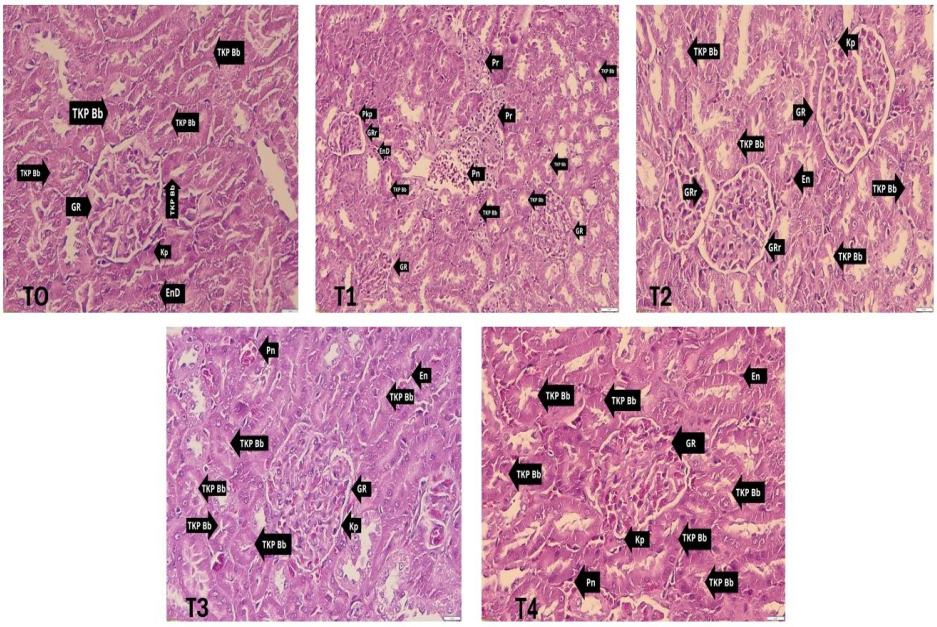

Figure 2: Effect of *B. pilosa* on histopathological alteration of kidney tissues in alcohol-induced CKI. T0 (CMC 0.5%); T1 (30 % alcohol 10 ml /kg); T2 (30 % alcohol 10 ml /kg + EEBP 250 mg /kg); T3 (30 % alcohol 10 ml /kg + EEBP 500 mg /kg); T4 (30 % alcohol 10 ml /kg + EEBP 750 mg /kg). GR: glomerulus, Kp: bowman's capsule, TKP Bb: proximal tubule, End: endothelial, Pr: inflammatory cells, Pn: inflammatory cells, BB: renal proximal tubular brush border, GRr: Glomerulus Retraction.

(a)

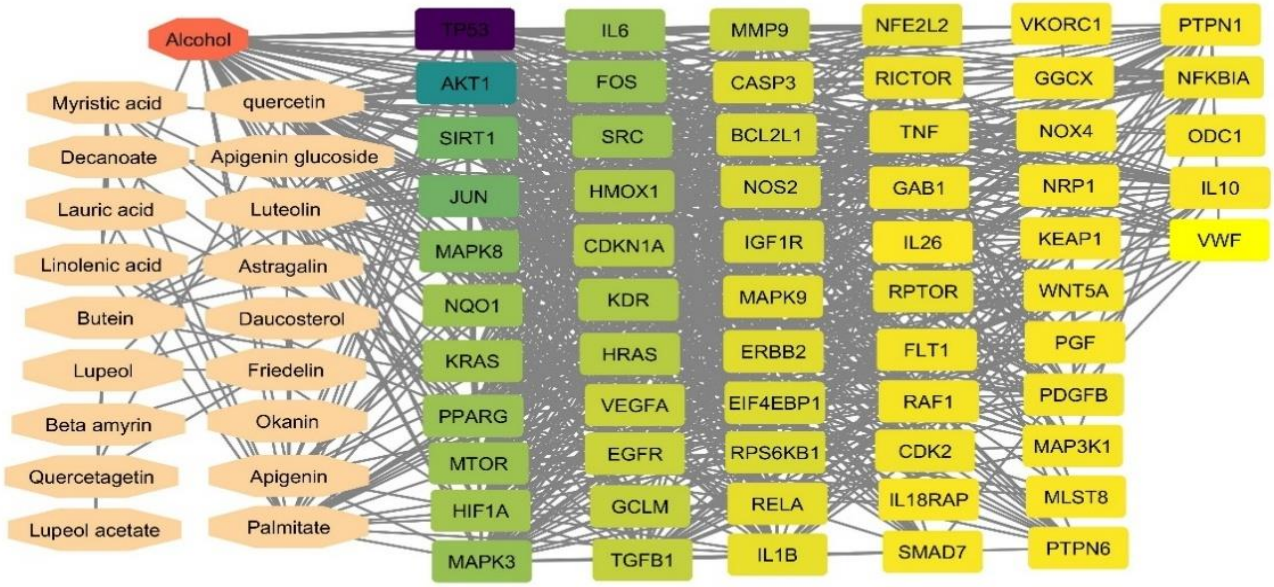

(b)

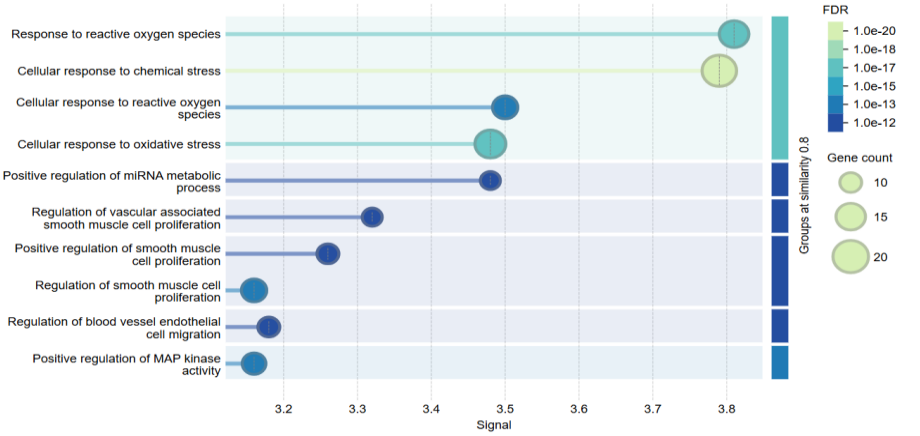

ISSN 2616-0684 (Print)
ISSN 2616-0692 (Electronic)

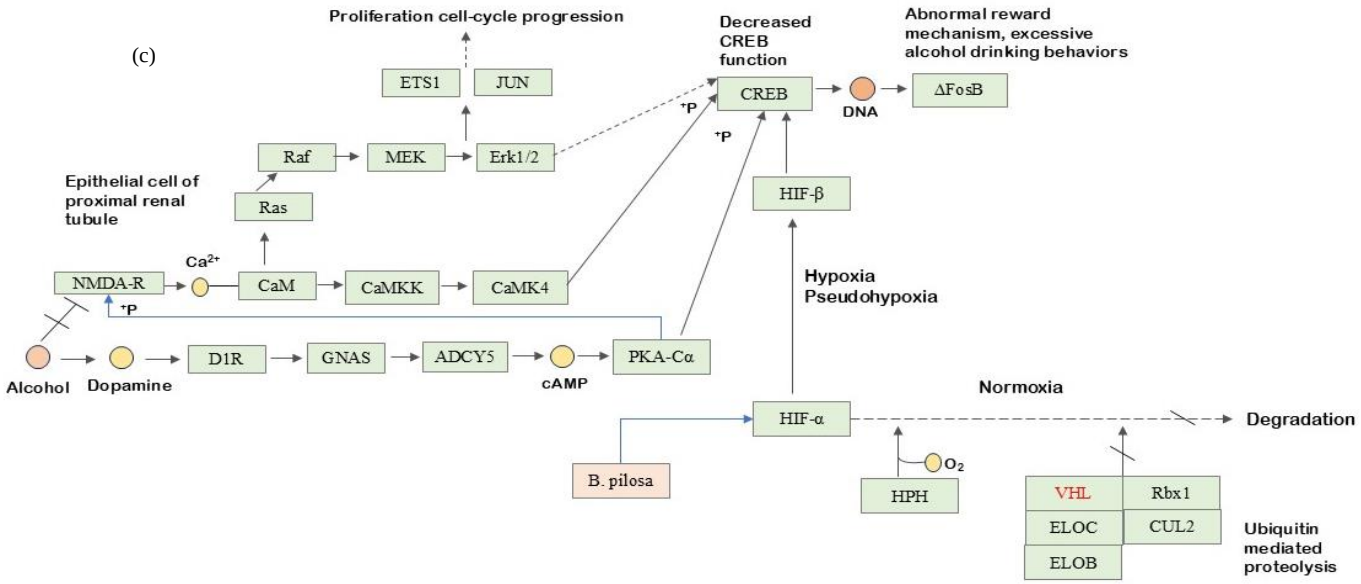

Figure 3: (a) Network pharmacology highlighting *B. pilosa* alleviates chronic kidney injury in alcoholic rats; (b) Enrichment analysis identifying significant biological activity of B. pilosa; (c) KEGG pathway illustrating the mechanism of B. pilosa against alcohol induced chronic kidney injury

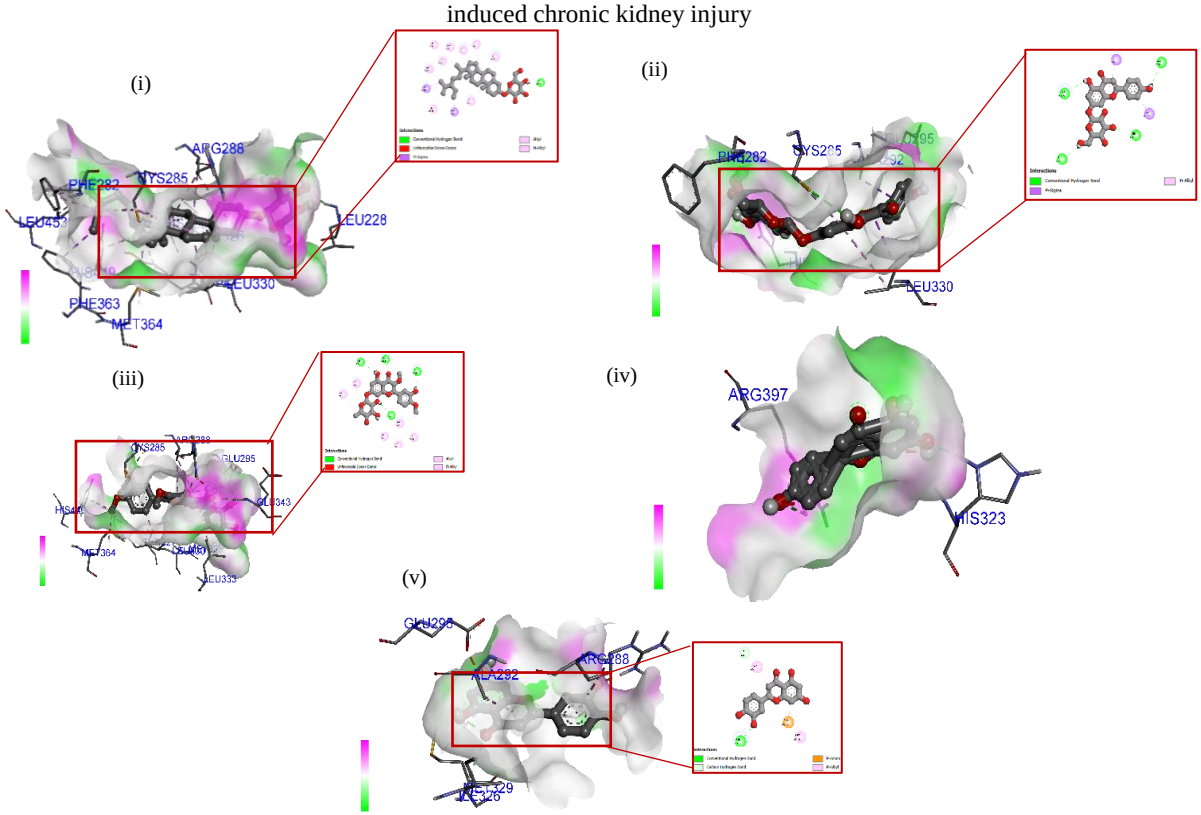

Figure 4A: Docking studies between PPARG and phytochemical from *B. pilosa* (i) Daucosterol; (ii)Apigenin-7-apioglucoside; (iii) Quercetin; (iv) Apigenin; (v) Luteolin.

ISSN 2616-0684 (Print)
ISSN 2616-0692
(Electronic)

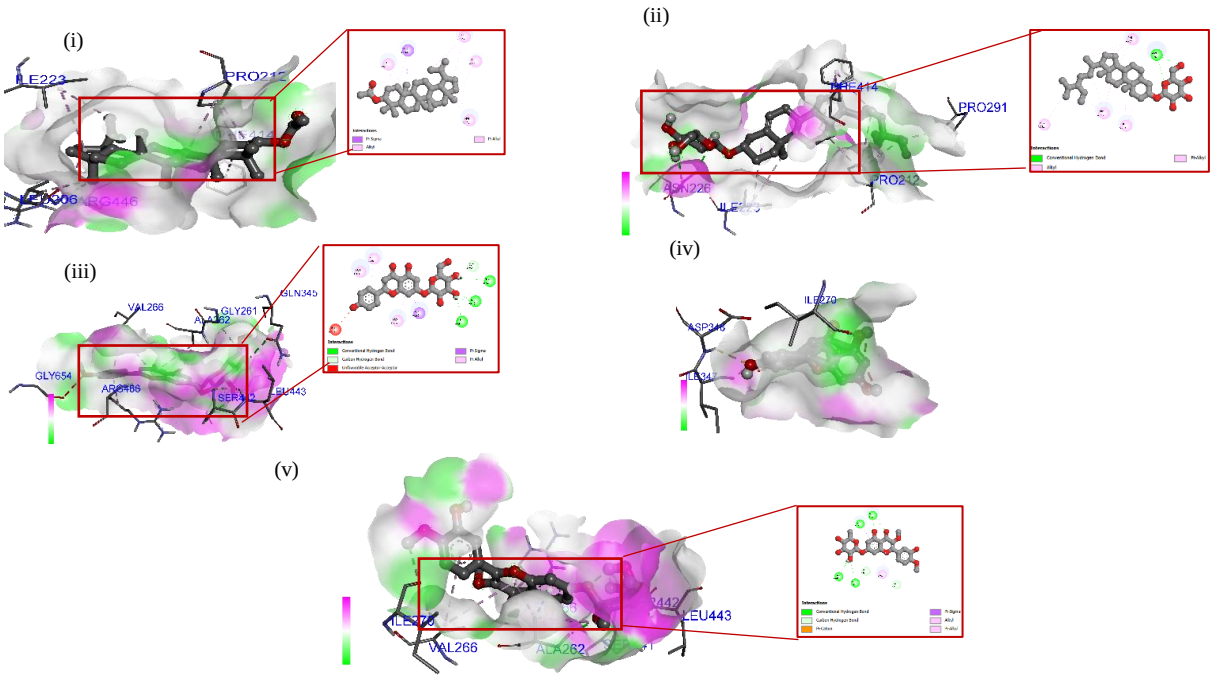

Figure 4B: Visualization of binding sites between SIRT and active compounds from *B. pilosa* (i) Lupeol acetate; (ii) Daucosterol; (iii) Apigenin-7-apioglucoside; (iv) Apigenin; (v) Quercetin.

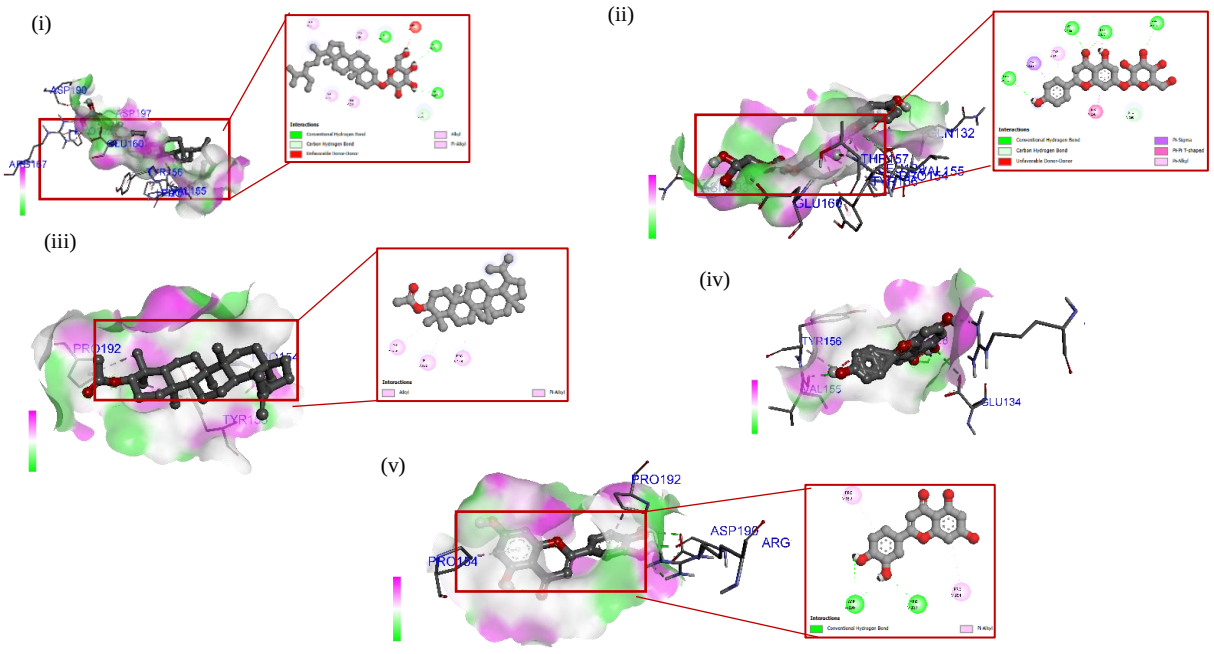

Figure 4C: Docking analysis between HIF1A and bioactive compounds of *B. pilosa* (i) Daucosterol; (ii)Apigenin-7-apioglucoside; (iii) Lupeol acetate; (iv) Apigenin; (v) Luteolin

ISSN 2616-0684 (Print)
ISSN 2616-0692 (Electronic)

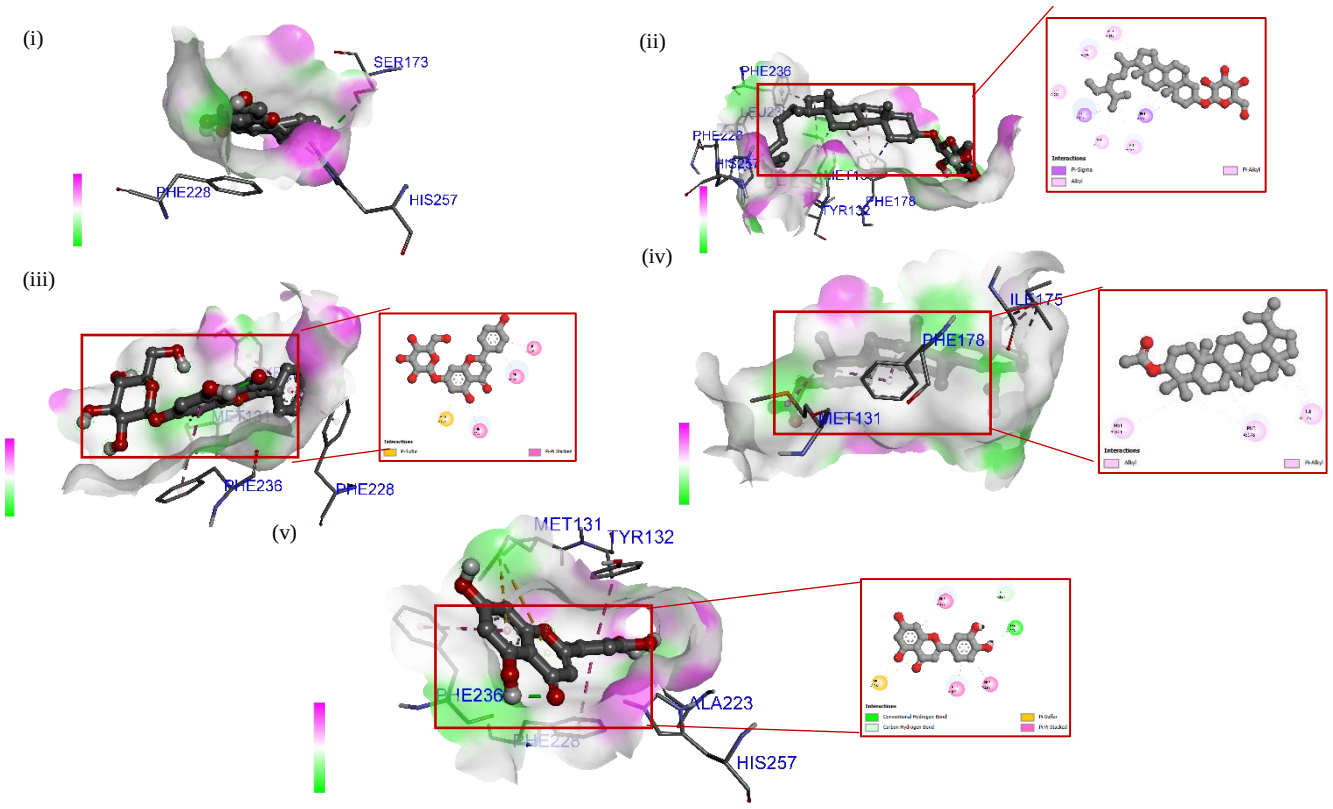

Figure 4D: Molecular docking between NQO1 and phytocompound of *B. pilosa* (i) Apigenin; (ii)Daucosterol; (ii)Apigenin-7-apioglucoside; (iv) Lupeol acetate; (v) Luteolin

Table 1: Docking results of all phytocompounds of *B. pilosa* binding to the target protein linked to alcoholic kidney injury

Compound	PPARG			SIRT			HIF1A			NQO1		
	Binding Affinity (kcal/mol)	Hydrogen Bond	Hydrophobic Interaction	Binding Affinity (kcal/mol)	Hydrogen Bond	Hydrophobic Interaction	Binding Affinity (kcal/mol)	Hydrogen Bond	Hydrophobic Interaction	Binding Affinity (kcal/mol)	Hydrogen Bond	Hydrophobic Interaction
Apigenin	-9.2	Met463	Leu453, Lys457	-8.5	Ile347, Asp348	Ala262, Ile270, Phe273	-7.6	Asn85, Ser86, Glu134, Val155	Leu129, Val155	-10.5	Ser173, His177, Ala223	Phe228
Apigenin-7-apioglucoside	-9.7	Phe282, Ser289, Glu295, His323, His449	Ala292, Met329	-8.8	Ala262, Gln345, Ser441, Ser442, Leu443, Arg466, Asp481	Val266, Arg274, Arg466	-8.1	Gly127, Gln132, Val155, Thr157, Arg167, Asn193	Leu129, Pro154, Glu160	-8.2	Tyr132, Phe236	Phe228
Butein	-7.8	Gln454, Glu460, Met463, Asp475	Val450, Leu453, Ile456, Lys457, Met463, Leu465, Tyr473	-7.6	Gly480, Cys482	Ala262	-7.2	Gly127, Val155, Thr157, Asp190, Asp197	Tyr156, Thr157, Pro192	-7.4	Ala223, His257	Leu230

ISSN 2616-0684 (Print)
ISSN 2616-0692 (Electronic)

Okanin	-8.0	Gln454, Ile456, Met463, Asp475	Val450, Leu453, Lys457, Tyr473	-8.3	Ile270, Asn465, Arg466, Gly480, Cys482	Ala262, Val266, Arg466	-6.8	Tyr83, Asn85, Ser86, Gly127, Leu128	Leu129, Pro154, Val155	-7.2	Ala223, His257	Tyr132, Leu230
Centaureidin	-8.1	Arg288, Glu295, Ser342, Glu343	Arg288, Ile326, Leu330	-7.5	Lys408	Glu410, Val412, Pro419	-6.9	Asp126, GLy127, Val155, Thr157, Gln164	Tyr156, Glu160	-6.6	Phe116	Phe178
Daucosterol	-10.4	Leu228, Glu343	Phe282, Gln286, Leu333, Phe363, Leu453, Leu469, Tyr473	-9.3	Asn226	Pro212, Ile223, Asp298, Phe414	-8.4	Arg167, Asp190, Asn193, Asp197, Arg200	Thr84, Leu129, Pro154, Val155, Tyr156	-9.2	Phe120	Tyr128, Met131, Tyr132, Phe178, Phe228, Leu230, Phe236
Luteolin	-8.5	Leu228, Arg288, Ser342	Phe226, Arg288, Ala292	-7.9	Lys304	Pro212, Ala295, Asp298, Tyr301	-7.5	Leu128, Arg167, Asp190	Pro154, Glu160	-7.9	Ala223, Phe236,	Phe228
Linolenic Acid	-6.5	-	Ile281, Phe282, Gln286, Ile326, Tyr327, Leu356, Phe360, Phe363, Phe453, Tyr473	-5.4	Ile210	Thr209, Pro212, Pro291, Gln294, Ala295, Phe414	-4.3	Glu134	Pro154, Tyr156, Thr157, Glu160, Pro192	-5.1	Ser71, Gly122	Pro68, Phe116, Glu117, Phe120, Tyr126, Ile175, Phe178
Lupeol acetate	-7.1	-	Tyr320, His323, Val446, Thr447, Gln454	-10.3	-	Leu206, Ile223, Pro291, Phe414	-7.7	-	Pro154, Tyr156, Pro192	-8.1	-	Phe116, Tyr128, Phe178, Phe232
Quercetagenin	-7.9	Ser289	Arg288, Glu291, Ile326	-7.3	Gln361, Glu416	Val412, Pro419	-6.7	Asn85, Ser86, Glu134, Val155, Arg200	Ile90, Leu129, Pro154, Val155	-6.7	Phe116, Gly174	Phe178
Quercetin	-9.7	Cys285, Arg288, Glu295, Ser342, Glu343	Leu330, Leu333	-8.3	Ala262, Asp272, Arg274, Ser275, Gly440, Ser442, Leu443, Arg 466	Ala262, Val266	-7.4	Arg120, His125, Gly127, Gln132, Val155, Thr157	Leu129, Pro192	-7.5	Phe120, Gly122, Tyr126, Gly174	Pro68, Phe178

ISSN 2616-0684 (Print)
ISSN 2616-0692 (Electronic)

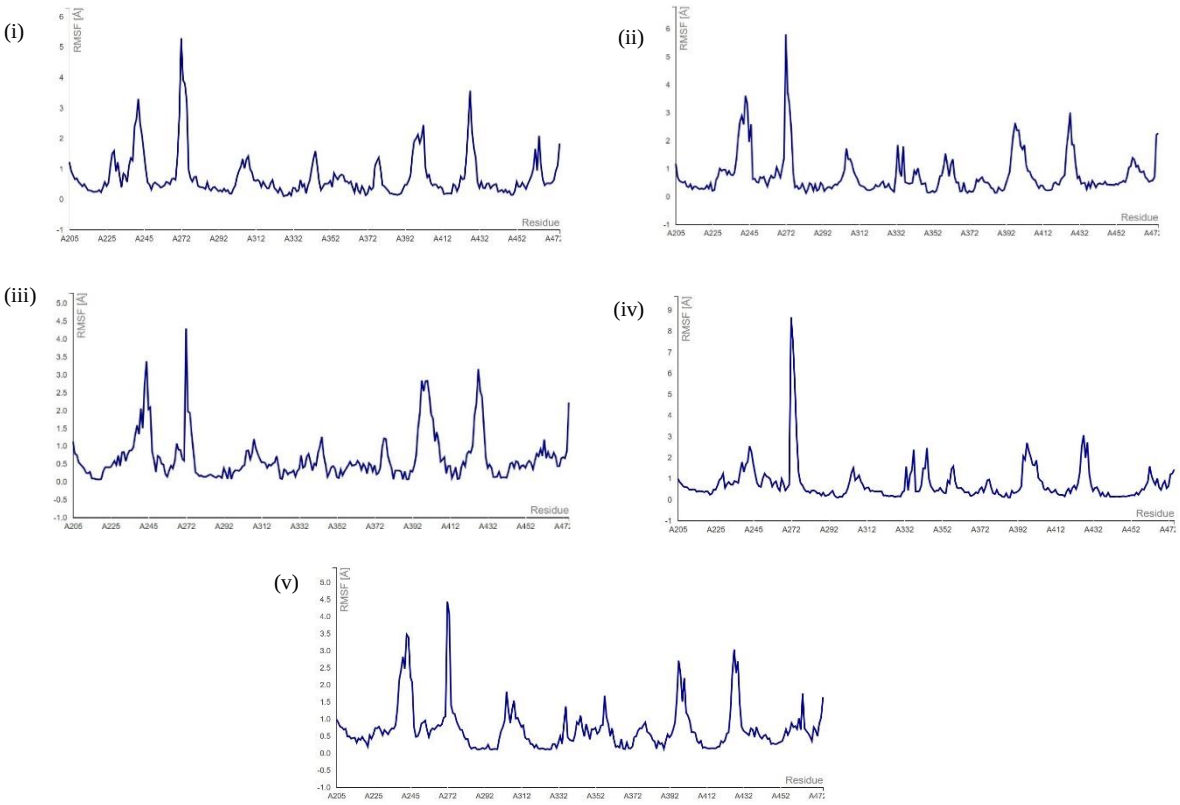

Figure 5A: RMSF plot of PPARG – the phytocompounds of *B. pilosa* for the structural flexibility analysis (i) Daucosterol; (ii)Apigenin-7-apioglucoside; (iii) Quercetin; (iv) Apigenin; (v) Luteolin.

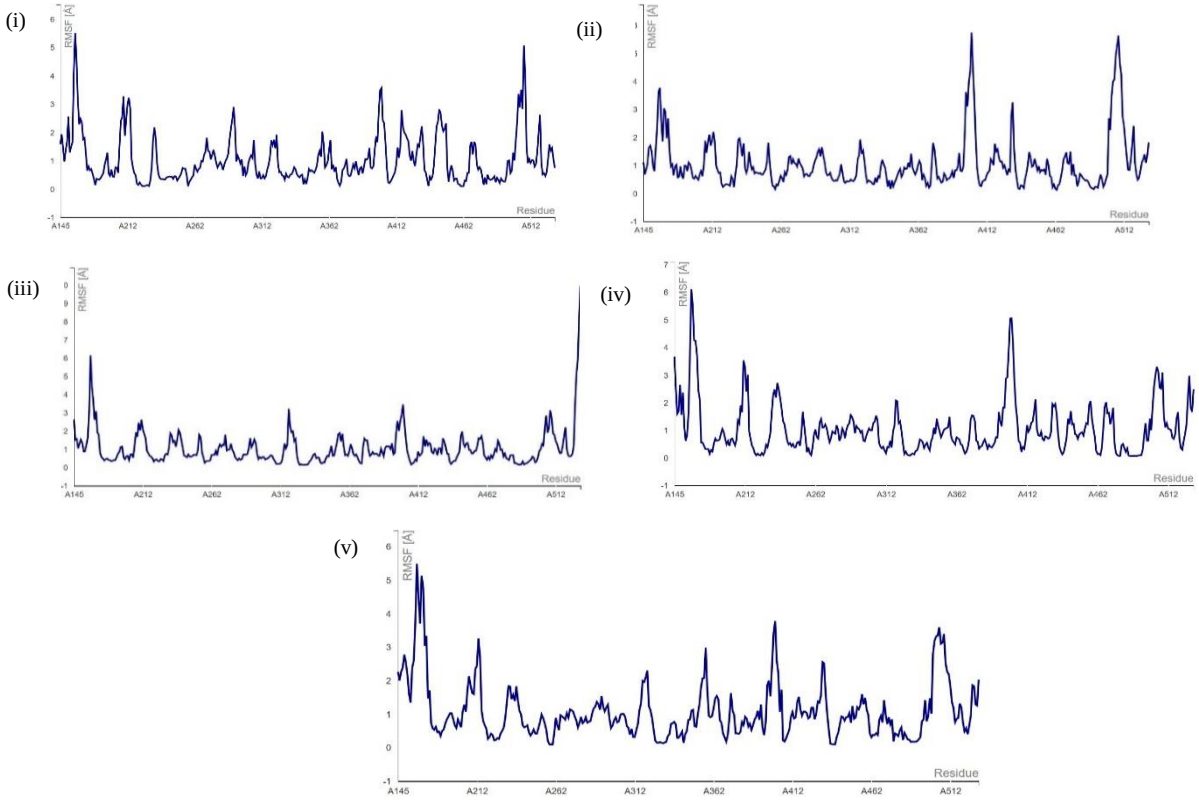

Figure 5B: The value of RMSF for the structural stability analysis between SIRT and the active compounds from *B. pilosa* (i) Lupeol acetate; (ii)Daucosterol; (iii) Apigenin-7-apioglucoside; (iv) Apigenin; (v) Quercetin

ISSN 2616-0684 (Print)
ISSN 2616-0692 (Electronic)

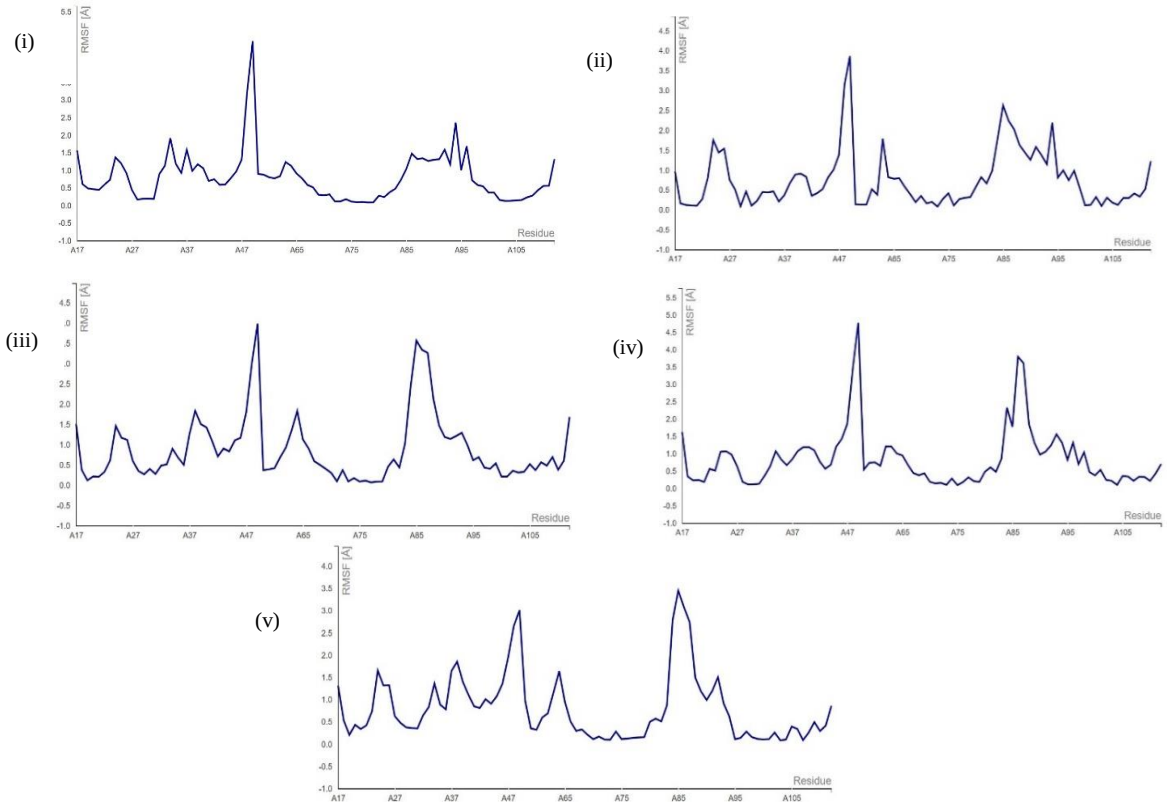

Figure 5C: The value of RMSF in the structural flexibility analysis between HIF1A and the active compounds from *B. pilosa* (i) Lupeol acetate; (ii)Daucosterol; (iii) Apigenin-7-apioglucoside; (iv) Apigenin; (v) Quercetin.

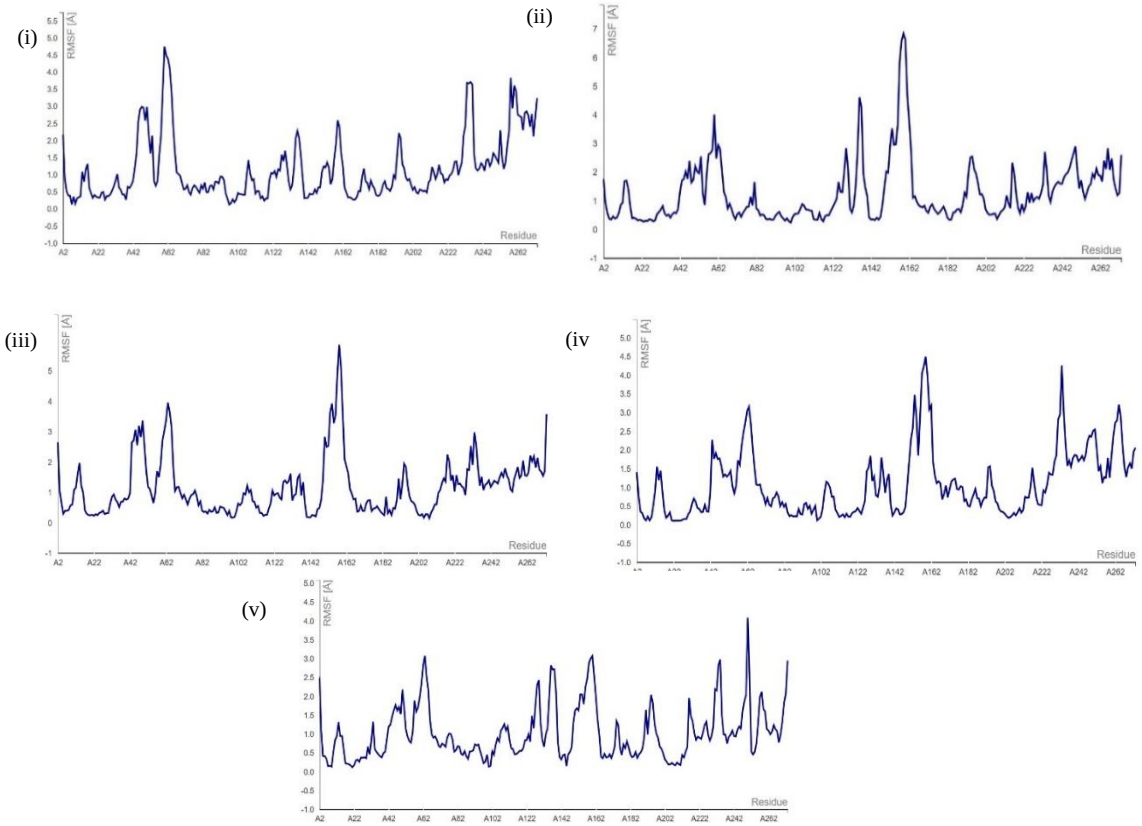

Figure 5D: The value of RMSF in the structural stability analysis between NQO1 and the active compounds from *B. pilosa* (i) Lupeol acetate; (ii)Daucosterol; (iii) Apigenin-7-apioglucoside; (iv) Apigenin; (v) Quercetin

Alcohol decreased the CREB (cAMP response element-binding protein) function through the PPARG and HIF signaling pathways, which promoted a high ROS level in epithelial cells of the proximal renal tubule.[42–44] Additionally, the oxidative stress generated mitochondrial dysfunction and elevated the lipid peroxidation mechanism[45,46] by decreasing the NAD+/NADH level in the alcoholic kidney.[47] The enhancement of SIRT expression could play a crucial role in encouraging the capacity of renal medullary interstitial cells to resist oxidative stress.[48] Further preclinical investigation is needed to examine the therapeutic effect of EEBP on oxidative stress markers in alcohol-induced CKI.

Conclusion

The findings unveil the therapeutic effect of *B. pilosa* in alcohol-induced chronic kidney injury through an integrative combining of pharmacoinformatic and *in vivo* studies. The histopathological analysis revealed that EEBP treatment could improve the damage in renal tissues. The administration of EEBP could maintain the biochemical parameters levels, such as total cholesterol, triglyceride, creatinine, uremic, HDL, and LDL, in alcohol kidney damage. The core genes, consisting of PPARG, SIRT, HIF1A, and NQO1, were involved in the mechanism of EEBP against alcoholic kidney injury through pharmacoinformatic approaches.

Conflict of interest

The authors declare no conflicts of interest.

Authors' Declaration

The authors hereby declare that the work presented in this article is original and that any liability for claims relating to the content of this article will be borne by them.

Acknowledgements

This work was funded by Institute for Research and Community Service (LPPM) of State University of Medan 0236/UN33.8/PPKM/PPT/2025.

References

1. Maharjan J, Le S, Green-Saxena A. Mortality, disease progression, and disease burden of acute kidney injury in alcohol use disorder subpopulation. Am J Med Sci 2022; 364: 46–52.
2. Kim G, Azmi L, Jang S. Aldehyde-alcohol dehydrogenase forms a high-order spirosome architecture critical for its activity. Nat. Commun. 2020; 10: 4527.
3. Ifechukwu J. Obiesie, Darlington N. Onyejike, Ifeoma M. Onyejike. Toxicological Evaluation of Co-Administration of Odogwu Bitters and Goko Cleanser Herbal Drinks on the Kidney of Adult Male Wistar Rats. Trop. J. Nat. Prod. Res. 2025; 9: 1256 – 1262.
4. Lee Y-J, Cho S, Kim SR. Effect of alcohol consumption on kidney function: population-based cohort study. Sci. Rep. 2021; 11: 2381.
5. Kuczyńska J, Nieradko-Iwanicka B. Comparison of the effects of ketoprofen and ketoprofen lysine salt on the Wistar rats' nervous system, kidneys and liver after ethyl alcohol intoxication. Biomed. & Pharmaco. 2023; 161: 114456.
6. Nour-Eddine Loud, Achraf Hamik, Rania Jerada. Evaluation of the Acute Diuretic Activity and Acute Toxicity of Hydroethanol Extract of the Fruits of *Ammodaucus leucotrichus*. Trop. J. Nat. Prod. Res. 2025; 9: 4775 – 4783.
7. Kayhan M, Vouillamoz J, Rodriguez DG. Intrinsic TGF-β signaling attenuates proximal tubule mitochondrial injury and inflammation in chronic kidney disease. Nat. Commun. 2023; 14: 3236.
8. Zhao C, Wang S, Zhai Y. Direct inhibition of human and rat 11β-hydroxysteroid dehydrogenase 2 by per- and polyfluoroalkyl substances: Structure-activity relationship and in silico docking analysis. Toxicol. 2023; 488: 153484.
9. Nishiyama M, Iwasaki Y, Nakayama S. Tissue-specific regulation of 11β hydroxysteroid dehydrogenase type-1 mRNA expressions in Cushing's syndrome mouse model. Steroids 2022; 183: 109021.
10. Su X, Bai M, Shang Y. Slc25a21 in cisplatin-induced acute kidney injury: a new target for renal tubular epithelial protection by regulating mitochondrial metabolic homeostasis. Cell Death Dis. 2024; 15: 891.
11. Ho HTT, Nguyen TH, Nguyen HH. Clinical significance of uric acid, blood pressure anticipating proteinuria worsening in pregnant women of advanced age. Endocr. Metabol. Sci. 2025; 19: 100273.
12. Tanaka A, Yamaguchi M, Ishimoto T. Association of alcohol consumption with the incidence of proteinuria and chronic kidney disease: a retrospective cohort study in Japan. Nutr. J. 2022; 21: 31.
13. Chen I-C, Tsai W-C, Hsu L-Y. Association between alcohol consumption and chronic kidney disease: a population-based survey. Clin. Exp. Nephrol. 2024; 28: 1121–1133.
14. Nguyen THD, Vu DC, Hanh PQP. Comparative analysis of phenolic content and *in vitro* bioactivities of *Bidens pilosa* L. flowers and leaves as affected by extraction solvents. J. Agric. Food. Res. 2023; 14: 100879.
15. Moharram BA, Al-Maqtari T, Alomaisi SAMA. Exploring the bioactive compounds and anticoagulant effects of *Bidens pilosa* cultivated in yemen through chromatographic and molecular docking approaches. Pharmacol. Res. – Nat. Prod. 2025; 6: 100174.
16. Pfoze BK, Singh RR, Pekosii BK. Phytochemical screening and assessment of the in-vitro wound healing activity of *Bidens pilosa* leaves. Pharmacol. Res. Nat. Prod. 2025; 8: 100331.
17. Rodríguez-Mesa XM, Contreras Bolaños LA, Mejía A. Immunomodulatory Properties of Natural Extracts and Compounds Derived from *Bidens pilosa L.*: Literature Review. Pharm. 2023; 15: 15051491.
18. Ekholm M, Aulbach M, Walsh S. Behavioral interventions targeting treatment adherence in chronic kidney disease: A systematic review and meta-analysis. Soc. Sci. Med. 2025; 366: 117594.
19. Wang H, Zhang J, Wang B. Identifying the natural compounds in *Jinqian Xuduan* Decoction for simultaneous uric acid lowering and chronic kidney disease amelioration. Phytomed. 2025; 146: 157109.
20. Sinaga E, Hasanah U, Sipahutar FRP. Chemopreventive potential of *Saurauia vulcani korth* in improving Rhodamine B induced hepato-renal carcinoma in Rats. Pharmacol. Res. – Mod. Chin. Med. 2023; 9: 100336.
21. Sinaga E, Silitonga M, Hasanah U. *Saurauia vulcani korth* against hepato-renal carcinoma integrated spleen damage in rats induce Rhodamine B: *In vivo* and *in silico*. AISTSSE 2024; 1:145–151.
22. Shu H, Peng Y, Hang W. Trimetazidine enhances myocardial angiogenesis in pressure overload-induced cardiac hypertrophy mice through directly activating Akt and promoting the binding of HSF1 to VEGF-A promoter. Acta Pharmacol. Sin. 2022; 43: 2550–2561.
23. Wróblewski K, Kmiecik S. Integrating AlphaFold pLDDT Scores into CABS-flex for enhanced protein flexibility simulations. Comput. Struct. Biotechnol. J. 2024; 23: 4350–4356.
24. Sinaga E, Hasanah U, Sipahutar FRP. Identifying therapeutic effect of kombucha Pirdot (*Saurauia vulcani Korth.*) against colorectal cancer: The experimental data and in silico approach. Med. in Microecol. 2024; 20: 100105.
25. Lin F, Luo S, Tu H. Association between alcohol consumption and renal function in patients with diabetes mellitus and

hypertension: insights from the Taiwan Biobank. BMC Nephrol 2025; 26: 256.
26. Silitonga M, Sidabutar H, Pranoto H. Protective effects of *Bidens pilosa* alleviates against alcohol—induced hepatic steatosis in rats: In vivo studies and in silico analysis. Pharmacol. Res.- Mod. Chin. Med. 2024; 13: 100546.
27. Kang H, Park Y-K, Lee J-Y. Inhibition of alcohol-induced inflammation and oxidative stress by astaxanthin is mediated by its opposite actions in the regulation of sirtuin 1 and histone deacetylase 4 in macrophages. BBA Mol. Cell Biol. Lipids 2021; 1866: 158838.
28. Proskynitopoulos PJ, Rhein M, Petersson LP. Differences in the promoter methylation of atrial natriuretic peptide and vasopressin in alcohol use disorder. A longitudinal case-control-study during withdrawal therapy. Psychoneuroendocrin. 2021; 133: 105387.
29. Sailer CO, Refardt J, Bissig S. Effects of alcohol consumption on copeptin levels and sodium-water homeostasis. Am. J. Physiol. Renal Physiol. 2020; 318: 702–709.
30. Jäckel M, Aicher N, Rilinger J. Incidence and predictors of delirium on the intensive care unit in patients with acute kidney injury, insight from a retrospective registry. Sci. Rep. 2021; 11: 17260.
31. Alharbi S, Aldubayan MA, Alhowail AH. Co-abuse of amphetamine and alcohol harms kidney and liver. Sci. Rep. 2024; 14: 23400.
32. Li Y, Zhu B, Song N. Alcohol consumption and its association with chronic kidney disease: Evidence from a 12-year China health and Nutrition Survey. Nutr, Metab and Cardiovasc Dis. 2022; 32: 1392–1401.
33. Catherine IO Ukam, Ugochukwu G Jidere, Josephine E. Egbung. Antioxidant Potentials of *Terminalia catappa* Seed Extract and Metformin on the Liver and Kidney of Diabetic Wistar Rats. Trop. J. of Nat. Prod. Res. 2025; 9(5): 2061-2066.
34. Li J, Shi X, Chen Z. Aldehyde dehydrogenase 2 alleviates mitochondrial dysfunction by promoting PGC-1α-mediated biogenesis in acute kidney injury. Cell Death Dis 2023; 14: 45.
35. Chen H, Hu Q, Lu Z. Aldehyde dehydrogenase 2 attenuates renal injury through inhibiting CYP4A expression. Trans. Res. 2025; 277: 1–12.
36. 45. Wang Y, Li K, Zhao W. Aldehyde dehydrogenase 3B2 promotes the proliferation and invasion of cholangiocarcinoma by increasing Integrin Beta 1 expression. Cell Death Dis. 2021; 12: 1158.
37. Tan D, Miao D, Zhao C. N6-methyladenosine-modified ALDH9A1 modulates lipid accumulation and tumor progression in clear cell renal cell carcinoma through the NPM1/IQGAP2/AKT signaling pathway. Cell Death Dis 2024; 15: 520.
38. Yokus B, Maccioni L, Fu L. The Link between Alcohol Consumption and Kidney Injury. Am. J Pathol. 2025; 6 : 11.
39. Alam F, Syed H, Amjad S. Interplay between oxidative stress, SIRT1, reproductive and metabolic functions. Curr Res Physiol 2021; 4: 119–124.